

Side-on Bound Diazene and Hydrazine Complexes of Ruthenium

Leslie D. Field,*[†] Hsiu L. Li,[†] and Scott J. Dalgarno[‡]

[†]*School of Chemistry, University of New South Wales, NSW 2052, Australia, and* [‡]*School of EPS-Chemistry, Heriot-Watt University, Edinburgh, Scotland EH14 4AS, U.K.*

Received April 28, 2010

The reaction of *cis*-[RuCl₂(PP)₂] (PP = depe, dmpe) with hydrazine afforded end-on bound ruthenium(II) hydrazine complexes. Treatment of the hydrazine complexes with strong base afforded the side-on bound ruthenium(0) diazene complexes *cis*-[Ru(η²-NH=NH)(PP)₂]. Treatment of *cis*-[Ru(η²-NH=NH)(depe)₂] with weak acid under chloride-free conditions afforded the side-on bound hydrazine complex *cis*-[Ru(η²-N₂H₄)(depe)₂]²⁺. These are the first reported side-on bound diazene and hydrazine complexes of ruthenium, and they have been characterized by NMR spectroscopy (¹H, ³¹P, ¹⁵N) and by X-ray crystallography. The interconversion between the ruthenium diazene and the ruthenium hydrazine by acid–base treatment was reversible.

Introduction

Recent progress toward the elucidation of the mechanism of the enzyme nitrogenase¹ has highlighted the importance of hydrazine² and diazene³ as intermediates in the reduction cascade of dinitrogen to ammonia. Diazene is a very reactive molecule which, in the free state, has a lifetime of minutes at room temperature.⁴ Diazene can be stabilized by complexation to transition metals, and there are now several examples of metal complexes with diazene in end-on⁵ and bridging⁶ coordination modes. We recently reported the synthesis of the first side-on bound diazene complex *cis*-[Fe(η²-NH=NH)(dmpe)₂] by reduction of the side-on bound hydrazine complex *cis*-[Fe(η²-N₂H₄)(dmpe)₂]²⁺ with potassium graphite.⁷ The iron diazene complex can be synthesized in better yield and purity by deprotonation of the hydrazine complex with a

strong base.⁸ We now report the formation of side-on bound diazene complexes of ruthenium by base treatment of ruthenium hydrazine complexes. Ruthenium, like iron, is an important catalyst component for some industrial processes for ammonia synthesis,⁹ and ruthenium is often regarded as a potentially more important metal in nitrogen reduction because it is able to bind dinitrogen and N₂H_x species more strongly than iron.¹⁰

Results and Discussion

Chloro Hydrazine Complexes of Ruthenium. The complexes *trans*-[RuCl₂(PP)₂] (PP = depe (1,2-bis(diethylphosphino)ethane), dmpe (1,2-bis(dimethylphosphino)ethane)) do not react with hydrazine even after prolonged reaction times and heating indicating that the chloride ligand is relatively tightly bound to ruthenium in the *trans* isomers. The chloride ligands of the *cis* isomers *cis*-[RuCl₂(PP)₂] were more labile presumably because of the influence of the *trans* phosphine ligands in these complexes.

Reaction of *cis*-[RuCl₂(depe)₂] with excess hydrazine in tetrahydrofuran resulted in the substitution of one chloride ligand with hydrazine to afford the ruthenium(II) complex with an end-on bound hydrazine ligand *cis*-[RuCl(η¹-N₂H₄)(depe)₂]⁺ **1** as the chloride salt (Scheme 1). Complex **1** was isolated as the tetraphenylborate salt, *cis*-[RuCl(η¹-N₂H₄)(depe)₂]⁺BPh₄⁻, **1**, on treatment with

*To whom correspondence should be addressed. E-mail: l.field@unsw.edu.au.

(1) Seefeldt, L. C.; Hoffman, B. M.; Dean, D. R. *Annu. Rev. Biochem.* **2009**, *78*, 701.

(2) Barney, B. M.; Yang, T.-C.; Igarashi, R. Y.; Dos Santos, P. C.; Laryukhin, M.; Lee, H.-I.; Hoffman, B. M.; Dean, D. R.; Seefeldt, L. C. *J. Am. Chem. Soc.* **2005**, *127*, 14960.

(3) Barney, B. M.; McClead, J.; Lukoyanov, D.; Laryukhin, M.; Yang, T.-C.; Dean, D. R.; Hoffman, B. M.; Seefeldt, L. C. *Biochemistry* **2007**, *46*, 6784.

(4) Back, R. A. *Rev. Chem. Intermed.* **1984**, *5*, 293.

(5) Cheng, T.-Y.; Ponce, A.; Rheingold, A. L.; Hillhouse, G. L. *Angew. Chem., Int. Ed. Engl.* **1994**, *33*, 657. You, Y.-S.; Lee, G.-H.; Peng, S.-M. *J. Chin. Chem. Soc. (Taipei)* **1996**, *43*, 261.

(6) Huttner, G.; Gartzke, W.; Allinger, K. *J. Organomet. Chem.* **1975**, *91*, 47. Sellmann, D.; Soglowek, W.; Knoch, F.; Moll, M. *Angew. Chem., Int. Ed. Engl.* **1989**, *28*, 1271. Sellmann, D.; Friedrich, H.; Knoch, F.; Moll, M. *Z. Naturforsch., B: Chem. Sci.* **1994**, *49*, 76. Sellmann, D.; Blum, D. C. F.; Heinemann, F. W. *Inorg. Chim. Acta* **2002**, *337*, 1. Fujisawa, K.; Lehnert, N.; Ishikawa, Y.; Okamoto, K. *Angew. Chem., Int. Ed.* **2004**, *43*, 4944.

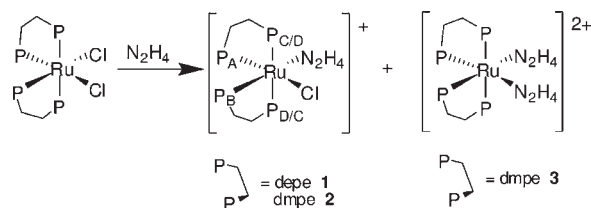
(7) Field, L. D.; Li, H. L.; Dalgarno, S. J.; Turner, P. *Chem. Commun.* **2008**, 1680.

(8) Field, L. D.; Li, H. L.; Magill, A. M. *Inorg. Chem.* **2009**, *48*, 5.

(9) Maxwell, G. R. *Synthetic Nitrogen Products, A Practical Guide to the Products and Processes*; Kluwer: New York, 2004; Aika, K.-i.; Tamaru, K. *Ammonia Synthesis over Non-Iron Catalysts and Related Phenomena in Ammonia Catalysis and Manufacture*; Nielsen, A., Ed.; Springer-Verlag: Berlin, 1995; pp 103–148.

(10) Mackay, B. A.; Fryzuk, M. D. *Chem. Rev.* **2004**, *104*, 385. Reiher, M.; Kirchner, B.; Hutter, J.; Sellmann, D.; Hess, B. A. *Chem.—Eur. J.* **2004**, *10*, 4443.

Scheme 1



NaBPh_4 in methanol. The $^{31}\text{P}\{^1\text{H}\}$ NMR spectrum of **1** contains four ddd signals (P_A 63.4 ppm, P_B 54.8 ppm, P_C 48.4 ppm, P_D 45.2 ppm), characteristic of an unsymmetrically substituted octahedral complex containing two depe ligands and two different ligands in *cis* coordination sites. A large coupling (279 Hz) is observed between two of the phosphorus atoms (P_C and P_D) indicating that these atoms are *trans* to each other in the coordination sphere. The two groups of hydrazine protons in the ^1H NMR spectrum at 4.42 and 3.74 ppm correlate to ^{15}N signals at -370.8 and -318.5 ppm, respectively, in a 2D ^1H – ^{15}N HSQC experiment indicating that the nitrogen atoms are in different environments. On labeling hydrazine with ^{15}N , an additional 28 Hz coupling is observed for P_B in the $^{31}\text{P}\{^1\text{H}\}$ NMR spectrum indicating that P_B corresponds to the atom *trans* to the hydrazine ligand. In the ^{15}N NMR spectrum, the highfield signal exhibits a reciprocal 28 Hz coupling to ^{31}P indicating that it corresponds to the metal-bound NH_2 . The highfield ^{15}N NMR signal also exhibits a 72 Hz coupling to the two nitrogen-bound protons as well as a 5 Hz ^{15}N – ^{15}N coupling to the other nitrogen atom. The ^{15}N resonance at lower field is broader and as it does not show any resolved coupling to ^{31}P , this corresponds to the non-coordinated NH_2 of the hydrazine unit.

Complex $\text{cis-}[\text{RuCl}(\eta^1\text{-N}_2\text{H}_4)(\text{depe})_2]^+ \mathbf{1}$ crystallizes as two different polymorphs **1a** (where diethyl ether was added to the reaction mixture to aid precipitation) and **1b** (no added diethyl ether) probably because of different crystal packing in the different mix of solvents used for crystallization. We discuss below the crystal structure of **1a**. Critical bond angles and bond lengths for **1b** are very similar and can be found in the Supporting Information.

The crystal structure of **1a** (Figure 1) confirms that the hydrazine ligand is bound in an end-on fashion with a Ru1-N1 bond length of 2.225(3) Å, which is significantly longer than those for other end-on bound Ru-hydrazine complexes reported in the literature (2.126(2)–2.165(3) Å). This is probably due to the stronger *trans* influence of the phosphine ligand compared to the arene as well as N- and S-containing ligands *trans* to the hydrazine ligand in the literature complexes (Table 1). The N2-N1 bond length of 1.461(4) Å is within the range reported for the other hydrazine complexes (1.378(10)–1.479(5) Å).

The analogous reaction of $\text{cis-}[\text{RuCl}_2(\text{dmpe})_2]$ with hydrazine in a mixture of tetrahydrofuran and methanol afforded the monosubstituted complex $\text{cis-}[\text{RuCl}(\eta^1\text{-N}_2\text{H}_4)(\text{dmpe})_2]^+ \mathbf{2}$ as the major product and the bis-substituted complex $\text{cis-}[\text{Ru}(\eta^1\text{-N}_2\text{H}_4)_2(\text{dmpe})_2]^{2+} \mathbf{3}$ as the minor product (Scheme 1). The chloride salts were precipitated from solution on addition of diethyl ether. Anion exchange to the tetraphenylborate salts was achieved by addition of NaBPh_4 to the chloride salts in

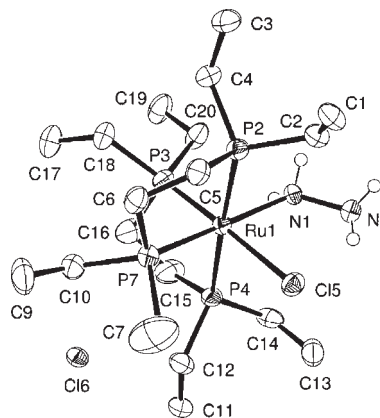


Figure 1. ORTEP plot of $\text{cis-}[\text{RuCl}(\eta^1\text{-N}_2\text{H}_4)(\text{depe})_2]^+ \mathbf{1a}$ (chloride salt, 50% displacement ellipsoids, carbon-bound hydrogen atoms have been excluded for clarity). Selected bond lengths (Å) and angles (deg): Ru1-N1 2.225(3), Ru1-P3 2.2837(11), Ru1-P7 2.3156(11), Ru1-P4 2.3474(11), Ru1-P2 2.3819(11), Ru1-Cl1 2.4937(11), N2-N1 1.461(4), N1-Ru1-P3 89.66(9), N1-Ru1-P7 173.86(9), N1-Ru1-P4 89.02(9), N1-Ru1-P2 90.69(9), N1-Ru1-Cl1 88.54(9), N2-N1-Ru1 120.4(2).

methanol. Separation of the mono- and disubstituted products **2** and **3** was achieved by selective extraction with tetrahydrofuran where the BPh_4 salt of **2** is significantly more soluble than the corresponding salt of **3**.

$\text{cis-}[\text{RuCl}(\eta^1\text{-N}_2\text{H}_4)(\text{dmpe})_2]^+ \mathbf{2}$ shows very similar NMR characteristics to $\text{cis-}[\text{RuCl}(\eta^1\text{-N}_2\text{H}_4)(\text{depe})_2]^+ \mathbf{1}$ including four ddd signals in the $^{31}\text{P}\{^1\text{H}\}$ NMR spectrum (P_A 51.6 ppm, P_B 43.8 ppm, P_C 40.5 ppm, P_D 33.9 ppm (thf- d_6)) and two signals in the ^{15}N NMR spectrum (Ru-NH_2 -369.2 ppm, NH_2 -320.7 ppm). In thf- d_6 , two broad ^1H resonances at 4.51 and 3.67 ppm are attributed to the Ru-NH_2 and the protons of the uncoordinated NH_2 respectively. In $\text{dms-}d_6$, the diastereotopic Ru-NH_2 protons appear as two broad multiplets at 5.29 and 4.66 ppm.

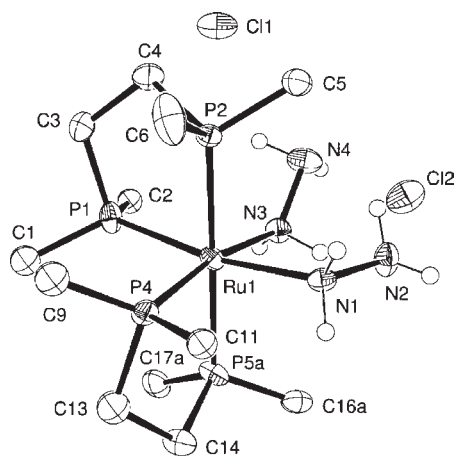
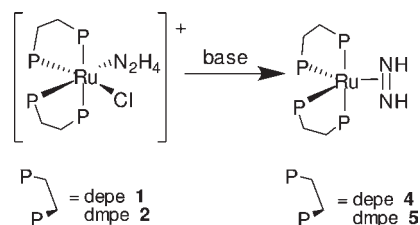
The $^{31}\text{P}\{^1\text{H}\}$ NMR spectrum of bis-hydrazine complex $\text{cis-}[\text{Ru}(\eta^1\text{-N}_2\text{H}_4)_2(\text{dmpe})_2]^{2+} \mathbf{3}$ contains two apparent triplets (splitting 20 Hz) characteristic of a symmetrically substituted octahedral complex containing two dmpe ligands and two identical ligands in *cis* coordination sites. The diastereotopic Ru-NH_2 protons resonate at 5.71 and 5.59 ppm, and both signals correlate to a single ^{15}N resonance at -368.0 ppm in the ^1H – ^{15}N HSQC experiment. The uncoordinated NH_2 proton signal appears as a broad resonance at 3.60 ppm and correlates to a ^{15}N resonance at -322.7 ppm. On labeling with ^{15}N , the lower field ^{31}P signal shows additional coupling to ^{15}N giving rise to a multiplet complicated by second order effects due to the symmetry of the molecule.

Crystals of $\text{cis-}[\text{Ru}(\eta^1\text{-N}_2\text{H}_4)_2(\text{dmpe})_2]^{2+} \mathbf{3}$ were obtained by careful layering of a solution of $\text{cis-RuCl}_2(\text{dmpe})_2$ and hydrazine in methanol/tetrahydrofuran with diethyl ether. The crystal structure of **3** (Figure 2) shows that both hydrazine ligands are bound in an end-on fashion with Ru-N bond lengths of 2.206(4) and 2.223(4) Å similar to that for $\text{cis-}[\text{RuCl}(\eta^1\text{-N}_2\text{H}_4)(\text{depe})_2]^+ \mathbf{1}$. The N-N bond lengths of 1.465(6) and 1.467(6) Å are also comparable to that observed for **1** above.

Diazeno Complexes of Ruthenium. Treatment of the hydrazine complex $\text{cis-}[\text{RuCl}(\eta^1\text{-N}_2\text{H}_4)(\text{depe})_2]^+ \mathbf{1}$ with KO^tBu or $\text{K}[\text{N}(\text{SiMe}_3)_2]$ in tetrahydrofuran afforded the side-on bound diazeno complex $\text{cis-}[\text{Ru}(\eta^2\text{-NH=NH})(\text{depe})_2] \mathbf{4}$ (Scheme 2). While there are a number of minor

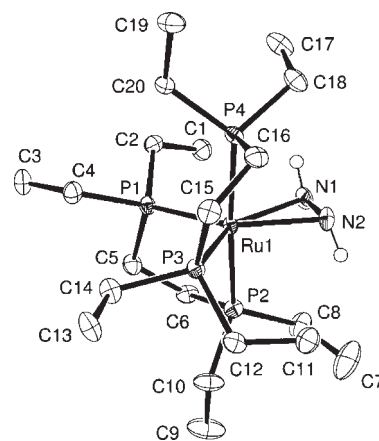
Table 1. Selected Bond Lengths for Previously Reported Ruthenium Hydrazine (End-on Bound) and Diazene Complexes

	Ru–N (Å)	N–N (Å)	ref.
Ruthenium End-on Bound Hydrazine Complexes			
Ru(η^6 -C ₆ H ₆)(S-2,6-Me ₂ C ₆ H ₃) ₂ (N ₂ H ₄)	2.143(7)	1.378(10)	11
Ru{(2-(3,5-Me ₂ C ₆ H ₃ N)C ₆ H ₄) ₂ S}(PMe ₃) ₂ (N ₂ H ₄)	2.165(3)	1.479(5)	12
Ru{2-SC ₆ H ₄ N(Me)CH ₂ } ₂ (PPh ₃)(N ₂ H ₄)	2.126(2)	1.449(2)	13
Ru{2,6-(2-SC ₆ H ₄ SCH ₂) ₂ -4-NEt ₂ py}(N ₂ H ₄)	2.1370(3)	1.4640(4)	14
Ru{2,6-(2-SC ₆ H ₄ SCH ₂) ₂ -4-NEt ₂ py}(N ₂ H ₄).N ₂ H ₄	2.137(4)	1.446(5)	14
Ruthenium Diazene Complexes			
{Ru(2-S-3,5-(^t Bu ₂ C ₆ H ₂)SCH ₂) ₂ (PPh ₃) ₂ }(μ -N ₂ H ₂)	2.009(8)	1.279(14)	15
{Ru(1,2-(2-SC ₆ H ₄) ₂ C ₆ H ₄)(PPh ₃) ₂ }(μ -N ₂ H ₂)	2.030(7)	1.29(1)	16
Ru(SPPPh ₂ NPPPh ₂ S)(PPh ₃)(N ₂ H ₂)	2.07(2)	1.235(av)	17
{Ru(2-SC ₆ H ₄ N(Me)CH ₂) ₂ (P ⁱ Pr ₃) ₂ }(μ -N ₂ H ₂)	1.994(5)	1.270(1)	18
{Ru(2-SC ₆ H ₄ N(Me)CH ₂) ₂ (P ⁱ Pr ₃)}(μ -N ₂ H ₂){Ru(2-(ClCH ₂ S)C ₆ H ₄ N(Me)(CH ₂) ₂ N(Me)C ₆ H ₄ S-2)Cl}	1.980(4)	1.279(5)	18

**Figure 2.** ORTEP plot of *cis*-[Ru(η^1 -N₂H₄)₂(dmpe)₂]²⁺ **3** (dichloride salt, 50% displacement ellipsoids, carbon-bound hydrogen atoms, atoms of less than 50% occupancy and hydrazine solvates have been excluded for clarity). Selected bond lengths (Å) and angles (deg): Ru1–N3 2.206(4), Ru1–N1 2.223(4), Ru1–P4 2.251(4), Ru1–P1 2.345(2), Ru1–P2 2.3587(13), Ru1–P5a 2.3504(14), N1–N2 1.465(6), N3–N4 1.467(6), N3–Ru1–N1 84.34(14), N3–Ru1–P4 169.12(14), N1–Ru1–P4 91.83(14), N3–Ru1–P1 90.77(11), N1–Ru1–P1 170.36(12), N3–Ru1–P5a 84.69(11), N1–Ru1–P5a 90.72(10), N3–Ru1–P2 95.62(11), N1–Ru1–P2 89.88(10), N2–N1–Ru1 116.0(2), N4–N3–Ru1 123.1(3).**Scheme 2**

byproducts in solution, complex **4** could be isolated by crystallization.

Crystals of [Ru(η^2 -NH=NH)(depe)₂] **4** suitable for X-ray crystallography were obtained by slow evaporation of a pentane solution under argon (Figure 3). The geometry of the complex is severely distorted in the equatorial plane where an acute angle of 38.78(13)° for N1–Ru1–N2 and angles of 109.08(11), 107.04(11), and 105.07(6) Å for N1–Ru1–P1, N2–Ru1–P3, and P1–Ru1–P3, respectively, were obtained. The Ru–N bond lengths of 2.123(4) and 2.134(3) Å are significantly longer

**Figure 3.** ORTEP plot of [Ru(η^2 -NH=NH)(depe)₂] **4** (50% displacement ellipsoids, carbon-bound hydrogen atoms have been excluded for clarity). Selected bond lengths (Å) and angles (deg): Ru1–N1 2.123(4), Ru1–N2 2.134(3), Ru1–P1 2.2734(15), Ru1–P3 2.2953(15), Ru1–P4 2.309(2), Ru1–P2 2.319(2), N1–N2 1.414(5), N1–Ru1–N2 38.78(13), N1–Ru1–P1 109.08(11), N2–Ru1–P1 147.74(9), N1–Ru1–P3 145.82(10), N2–Ru1–P3 107.04(11), P1–Ru1–P3 105.07(6), N1–Ru1–P4 90.91(11), N2–Ru1–P4 82.87(11), N1–Ru1–P2 84.94(11), N2–Ru1–P2 93.17(12), N2–N1–Ru1 71.03(19), N1–N2–Ru1 70.19(19).

than those reported for other Ru-diazene complexes in the literature (1.980(4)–2.07(2) Å, see Table 1). The N–N bond (1.414(5) Å) is significantly longer than those reported in the literature (1.235–1.29(1) Å, see Table 1) although similar to the N–N bond length reported for the iron diazene complex [Fe(η^2 -NH=NH)(dmpe)₂] (1.427(7) Å).⁷ In an analogous fashion to the related iron diazene complex, the lengthening of the N–N bond is consistent

(11) Mashima, K.; Kaneyoshi, H.; Kaneko, S.; Tani, K.; Nakamura, A. *Chem. Lett.* **1997**, 569.

(12) Takemoto, S.; Kawamura, H.; Yamada, Y.; Okada, T.; Ono, A.; Yoshikawa, E.; Mizobe, Y.; Hidai, M. *Organometallics* **2002**, *21*, 3897.

(13) Sellmann, D.; Hille, A.; Rosler, A.; Heinemann, F. W.; Moll, M. *Inorg. Chim. Acta* **2004**, *357*, 3336.

(14) Sellmann, D.; Shaban, S. Y.; Heinemann, F. W. *Eur. J. Inorg. Chem.* **2004**, 4591.

(15) Sellmann, D.; Kappler, J.; Moll, M.; Knoch, F. *Inorg. Chem.* **1993**, *32*, 960.

(16) Sellmann, D.; Engl, K.; Heinemann, F. W.; Sieler, J. *Eur. J. Inorg. Chem.* **2000**, 1079.

(17) Zhang, Q.-F.; Zheng, H.; Wong, W.-Y.; Wong, W.-T.; Leung, W.-H. *Inorg. Chem.* **2000**, *39*, 5255.

(18) Sellmann, D.; Hille, A.; Rosler, A.; Heinemann, F. W.; Moll, M.; Brehm, G.; Schneider, S.; Reiher, M.; Hess, B. A.; Bauer, W. *Chem.—Eur. J.* **2004**, *10*, 819.

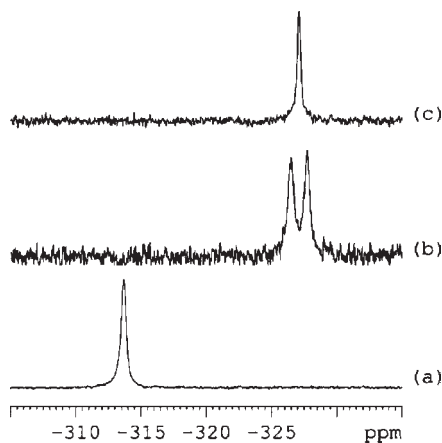


Figure 4. ^{15}N NMR spectra (41 MHz) of $[\text{Ru}(\eta^2\text{-NH=NH})(\text{depe})_2]$ **4** in $\text{thf-}d_8$ at (a) 298 K, (b) 200 K, and (c) 200 K, ^1H decoupled.

with back-bonding from the filled d-orbitals of ruthenium to the antibonding π^* orbitals of the diazene ligand.⁸ The H-N=N-H fragment is nearly planar, which indicates that the coordinated diazene is analogous to a coordinated alkene. The $^{31}\text{P}\{^1\text{H}\}$ NMR spectrum of $[\text{Ru}(\eta^2\text{-NH=NH})(\text{depe})_2]$ **4** contains two apparent triplets at 61.7 and 57.5 ppm, characteristic of a symmetrically substituted octahedral complex with two depe ligands and two identical donors in cis positions. The ^{15}N -labeled complex exhibits an additional 4 Hz splitting in the lower field ^{31}P signal and a broad resonance at -313.7 ppm in the ^{15}N NMR spectrum (Figure 4). The ^{15}N chemical shift is similar to those reported for $[\text{Fe}(\eta^2\text{-NH=NH})(\text{dmpe})_2]$ (-310.7 ppm)⁷ and $[\text{Fe}(\eta^2\text{-NH=NH})(\text{DMeOPrPE})_2]$ ($\text{DMeOPrPE} = 1,2\text{-bis}(\text{dimethoxypropylphosphino})\text{ethane}$) (-315.2 ppm).¹⁹ On cooling a $\text{thf-}d_8$ solution to 200 K, the proton-coupled ^{15}N spectrum appears as a doublet-like multiplet (the unresolved AA' portion of an $\text{AA}'\text{XX}'$ with an apparent splitting of approximately 52 Hz) and this collapses to a broad singlet on ^1H decoupling. This behavior is probably due to exchange (probably via rapid protonation/deprotonation) of the protons on the nitrogen atoms of the diazene unit, and this exchange is slowed sufficiently at low temperature such that the $^1\text{H-}^{15}\text{N}$ coupling and the resulting multiplicity can be observed.

Treatment of $\text{cis-}[\text{RuCl}(\eta^1\text{-N}_2\text{H}_4)(\text{dmpe})_2]^+$ **2** with KO^tBu in tetrahydrofuran afforded the corresponding side-on bound diazene complex $[\text{Ru}(\eta^2\text{-NH=NH})(\text{dmpe})_2]$ **5** (Scheme 2). A number of unidentified byproducts were formed in the reaction mixture; however, **5** was isolated in low yield by crystallization. Crystals suitable for X-ray crystallography were obtained by slow evaporation of a benzene- d_6 solution of **5** under argon (Figure 5). The geometry of the complex, as for **4**, is severely distorted in the equatorial plane with angles of $38.61(9)$, $109.68(5)$, and $102.04(4)^\circ$ for $\text{N}4^i\text{-Ru1-N4}$, N4-Ru1-P4 , and P4-Ru1-P4^i , respectively. The Ru-N and N-N bond lengths of $2.1589(15)$ and $1.427(3)$ Å are similar to those for **4**. The NMR features for complex **5** are also very similar to those for complex **4** including two apparent triplets in the $^{31}\text{P}\{^1\text{H}\}$ NMR spectrum (41.4 and 39.2 ppm) and one signal in the ^{15}N spectrum ($\delta -312.2$ ppm). As for

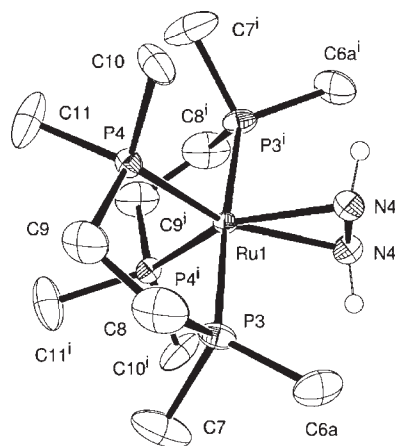


Figure 5. ORTEP plot of $[\text{Ru}(\eta^2\text{-NH=NH})(\text{dmpe})_2]$ **5** (50% displacement ellipsoids, carbon-bound hydrogen atoms and atoms of less than 50% occupancy have been excluded for clarity). The molecule has crystallographically imposed 2-fold symmetry. Selected bond lengths (Å) and angles (deg): Ru1-N4 2.1589(15), Ru1-P4 2.2904(8), Ru1-P3 2.3127(4), N4-N4^i 1.427(3), $\text{N4}^i\text{-Ru1-N4}$ 38.61(9), $\text{N4}^i\text{-Ru1-P4}$ 148.29(5), N4-Ru1-P4 109.68(5), P4-Ru1-P4^i 102.04(4), $\text{N4}^i\text{-Ru1-P3}^i$ 85.29(5), N4-Ru1-P3^i 91.73(5), $\text{N4}^i\text{-N4-Ru1}$ 70.69(4).

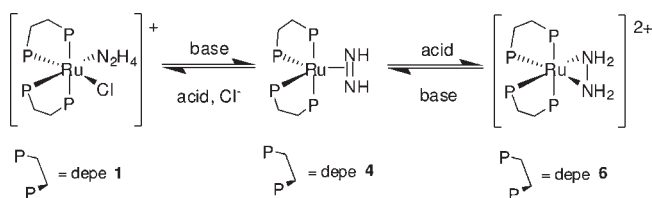
complex **4**, the proton-coupled ^{15}N signal is split into a doublet-like multiplet (splitting approximately 45 Hz) on cooling to 200 K.

Side-on Bound Hydrazine Complex of Ruthenium. When diazene complex $[\text{Ru}(\eta^2\text{-NH=NH})(\text{depe})_2]$ **4**, formed in situ by addition of KO^tBu to a solution of $[\text{RuCl}(\eta^1\text{-N}_2\text{H}_4)(\text{depe})_2]^+$ **1**, was treated with mild acid lutidinium triflate, the starting chloro hydrazine complex **1** reformed. However, treating diazene complex **4** that had been recrystallized from benzene/pentane (i.e., chloride-free) with lutidinium triflate afforded the side-on bound hydrazine complex $\text{cis-}[\text{Ru}(\eta^2\text{-N}_2\text{H}_4)(\text{depe})_2]^{2+}$ **6** as the bis-triflate salt (Scheme 3). Two apparent triplets at 70.7 and 50.1 ppm were observed in the $^{31}\text{P}\{^1\text{H}\}$ NMR spectrum characteristic of a symmetrically substituted octahedral complex with two depe ligands and two identical ligands in cis positions. Two broad ^1H resonances at 5.89 and 5.29 ppm correlated to a single ^{15}N signal at -378.7 ppm in a 2D $^1\text{H-}^{15}\text{N}$ HSQC experiment indicating the side-on bound nature of the hydrazine ligand. The ^{15}N chemical shift is similar to those reported for side-on hydrazine complexes $[\text{Fe}(\eta^2\text{-N}_2\text{H}_4)(\text{dmpe})_2]^{2+}$ (-387.9 ppm)⁷ and $[\text{Fe}(\eta^2\text{-N}_2\text{H}_4)(\text{DMeOPrPE})_2]^{2+}$ (-395.9 ppm).¹⁹ The protonation reaction to form the side-on bound hydrazine complex **6** is reversible as treatment with KO^tBu reformed the diazene complex **4**.

X-ray quality crystals of hydrazine complex $\text{cis-}[\text{Ru}(\eta^2\text{-N}_2\text{H}_4)(\text{depe})_2]^{2+}$ **6** were obtained from a tetrahydrofuran solution of diazene complex **4** and lutidinium tetrafluoroborate confirming the side-on configuration of the hydrazine ligand (Figure 6). The octahedral geometry of the molecule is severely distorted with an acute N2-Ru1-N1 angle of $39.26(6)^\circ$ and N2-Ru1-P4 , N1-Ru1-P2 , and P4-Ru1-P2 angles of $110.55(4)$, $114.70(4)$, and $95.748(18)^\circ$, respectively. The Ru-N bond lengths ($2.1594(16)$ and $2.1749(16)$ Å) are shorter than those for hydrazine complexes **1** ($2.225(3)$ Å) and **3** ($2.206(4)$ and $2.223(4)$ Å) although slightly longer than most of those reported previously ($2.126(2)$ – $2.165(3)$ Å, see Table 1). The N-N bond length ($1.456(2)$ Å) is similar to those for **1**

(19) Crossland, J. L.; Balesdent, C. G.; Tyler, D. R. *Dalton Trans.* **2009**, 4420.

Scheme 3



(1.461(4) Å) and **3** (1.465(6) and 1.467(6) Å) and well within the range of other hydrazine complexes (1.378(10)–1.479(5) Å, see Table 1).

Conclusions

We have developed a synthesis of ruthenium(0) diazene complexes by deprotonation of ruthenium(II) chloro hydrazine complexes. Acid treatment of a diazene complex in chloride-free conditions afforded a side-on bound hydrazine complex. The complexes were characterized spectroscopically (^1H , ^{15}N , and ^{31}P NMR) as well as by X-ray crystallography. To the best of our knowledge, the ruthenium diazene complexes $[\text{Ru}(\eta^2\text{-NH=NH})(\text{PP})_2]$ **4** and **5** and hydrazine complex $[\text{Ru}(\eta^2\text{-N}_2\text{H}_4)(\text{depe})_2]^{2+}$ **6** are the first side-on bound diazene and hydrazine complexes on ruthenium to be crystallographically characterized. The ruthenium diazene structures are comparable to the analogous iron diazene complex previously reported⁷ and the bonding is probably best considered a metal-coordinated π -complex similar to that in a metal-alkene. This binding mode is rare for diazene (so far only two examples are known and these are both on iron). Likewise, the η^2 -binding mode for hydrazine is rare, and there are no other examples of this binding mode at ruthenium. The observation that the ruthenium-bound diazene and hydrazine complexes can be interconverted reversibly by acid–base chemistry is complementary to previous work on iron^{8,19} and may lead to greater understanding of the mechanism of dinitrogen reduction on transition metals.

Experimental Section

All manipulations of metal complexes and air-sensitive reagents were carried out using standard Schlenk techniques or in nitrogen or argon filled glove boxes. Solvents were dried and distilled under nitrogen or argon from sodium/benzophenone (benzene) and dimethoxymagnesium (methanol). Tetrahydrofuran (inhibitor-free), diethyl ether, and pentane were dried and deoxygenated using a Pure Solv 400-4-MD (Innovative Technology) solvent purification system. 2-Methoxyethanol was deoxygenated before use. Deuterated solvents were purchased from Cambridge Isotope Laboratories. Tetrahydrofuran- d_8 , benzene- d_6 , and toluene- d_8 were dried over and distilled from sodium/benzophenone. Dimethyl sulfoxide- d_6 was dried over activated molecular sieves and deoxygenated with three freeze–pump–thaw cycles.

Hydrazine (1 M in tetrahydrofuran) was purchased from Aldrich and deoxygenated before use. Hydrazine- $^{15}\text{N}_2$ was prepared by Soxhlet extraction of $^{15}\text{N}_2\text{H}_4 \cdot \text{H}_2\text{SO}_4$ with liquid ammonia.²⁰ Potassium *t*-butoxide was sublimed twice and stored under an inert atmosphere. 2,6-Lutidinium triflate was prepared by reaction of equimolar amounts of 2,6-lutidine and triflic acid in toluene. 2,6-Lutidinium tetrafluoroborate was prepared by reaction of equimolar amounts of

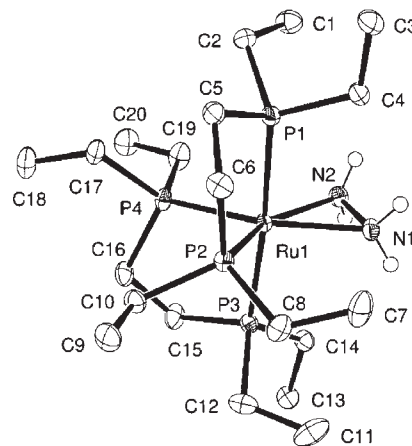


Figure 6. ORTEP plot of $[\text{Ru}(\eta^2\text{-N}_2\text{H}_4)(\text{depe})_2]^{2+}$ **6** (bis- BF_4 salt, 50% displacement ellipsoids, carbon-bound hydrogen atoms, BF_4 counterions and tetrahydrofuran solvate have been excluded for clarity). Selected bond lengths (Å) and angles (deg): Ru1–N2 2.1594(16), Ru1–N1 2.1749(16), Ru1–P4 2.2859(5), Ru1–P2 2.2984(5), Ru1–P1 2.3452(5), Ru1–P3 2.3851(5), N1–N2 1.456(2), N2–Ru1–N1 39.26(6), N2–Ru1–P4 110.55(4), N1–Ru1–P2 114.70(4), P4–Ru1–P2 95.748(18), N2–N1–Ru1 69.79(9), N1–N2–Ru1 70.95(9).

2,6-lutidine and tetrafluoroboric acid in diethyl ether. Dimethylphenylphosphine and potassium bis(trimethylsilyl)amide were purchased from Aldrich and used without further purification. 1,2-Bis(dimethylphosphino)ethane (dmpe) and 1,2-bis(diethylphosphino)ethane (depe) were purchased from Strem and used without further purification. $[\{\text{Ru}(\text{PMe}_2\text{Ph})_3\}_2(\mu\text{-Cl})_2]\text{Cl}$ was prepared by refluxing a solution of $\text{RuCl}_3 \cdot x\text{H}_2\text{O}$ and PMe_2Ph in 2-methoxyethanol.^{21,22} $[\text{RuCl}_2(\text{dmsO})_4]$ was prepared according to the literature method.²³ The complexes *cis*- $[\text{RuCl}_2(\text{dmpe})_2]$ and *cis*- $[\text{RuCl}_2(\text{depe})_2]$ were prepared by heating a mixture of $[\{\text{Ru}(\text{PMe}_2\text{Ph})_3\}_2(\mu\text{-Cl})_2]\text{Cl}$ and the appropriate bidentate phosphine ligand at 200 °C.^{21,24} *cis*- $[\text{RuCl}_2(\text{depe})_2]$ was also prepared from $[\text{RuCl}_2(\text{dmsO})_4]$ according to the literature method.^{24,25}

Air-sensitive NMR samples were prepared in argon or nitrogen filled glove boxes or on a high vacuum line by vacuum transfer of solvent into an NMR tube fitted with a concentric Teflon valve. ^1H , ^{31}P , ^{15}N , and ^{19}F NMR spectra were recorded on Bruker DRX400 or DPX300 NMR spectrometers at 298 K unless otherwise stated. ^1H NMR spectra were referenced to residual solvent resonances while ^{31}P spectra were referenced to external neat trimethyl phosphite at δ 140.85 ppm. ^{15}N NMR spectra were reference to external neat nitromethane at δ 0.0 ppm. ^{19}F NMR spectra were referenced according to the IUPAC unified scale using $\Xi_{\text{F}} = 94.094011$.²⁶ Simulation of ^{31}P spectra for *cis*-unsymmetrical complexes were performed iteratively using the simulation program NUMMRIT (SpinWorks 3), and the signs for coupling constants are not implied. Infrared spectra were recorded on a Nicolet Avatar 360 FTIR spectrometer as nujol mulls. Microanalyses were carried out at the Campbell Microanalytical Laboratory, University of Otago, New Zealand. Mass spectrometric analysis for this work was carried out at the Bioanalytical Mass Spectrometry Facility, UNSW.

(21) Chatt, J.; Hayter, R. G. *J. Chem. Soc.* **1961**, 896.

(22) Chatt, J.; Shaw, B. L.; Field, A. E. *J. Chem. Soc.* **1964**, 5507.

(23) Evans, I. P.; Spencer, A.; Wilkinson, G. *J. Chem. Soc., Dalton Trans.* **1973**, 204.

(24) The products contained varying amounts (5–30%) of trans isomers.

(25) Winter, R. F.; Brunner, B. M.; Scheiring, T. *Inorg. Chim. Acta* **2000**, 310, 21.

(26) Harris, R. K.; Becker, E. D.; Cabral de Menezes, S. M.; Granger, P.; Hoffman, R. E.; Zilm, K. W. *Pure Appl. Chem.* **2008**, 80, 59.

(20) Glassman, T. E.; Vale, M. G.; Schrock, R. R. *J. Am. Chem. Soc.* **1992**, 114, 8098. Smith, M. R.; Cheng, T. Y.; Hillhouse, G. L. *J. Am. Chem. Soc.* **1993**, 115, 8638.

Table 2. Crystallographic Data for Complexes 1, 3, 4, 5, and 6

	1a	1b	3	4	5	6
formula	C ₂₀ H ₅₂ Cl ₂ N ₂ P ₄ Ru	C ₄₀ H ₁₀₄ Cl ₄ N ₈ P ₈ Ru ₂	C ₁₂ H ₄₀ Cl ₂ N ₈ P ₄ Ru	C ₂₀ H ₅₀ N ₂ P ₄ Ru	C ₁₂ H ₃₂ N ₂ P ₄ Ru	C ₂₄ H ₆₀ B ₂ F ₈ N ₂ OP ₄ Ru
<i>M</i> (g mol ⁻¹)	616.49	1289.01	592.37	543.57	429.35	791.31
size (mm ³)	0.3 × 0.25 × 0.2	0.45 × 0.40 × 0.22	0.30 × 0.25 × 0.25	0.40 × 0.35 × 0.25	0.40 × 0.35 × 0.30	0.45 × 0.35 × 0.30
crystal morphology	colorless block	colorless block	colorless block	colorless block	colorless block	colorless block
crystal system	monoclinic	triclinic	monoclinic	orthorhombic	monoclinic	monoclinic
space group	<i>P</i> 2 ₁ / <i>n</i>	<i>P</i> $\bar{1}$	<i>P</i> 2 ₁ / <i>c</i>	<i>Pna</i> 2 ₁	<i>C</i> 2/ <i>c</i>	<i>P</i> 2 ₁ / <i>n</i>
<i>a</i> (Å)	10.3779(13)	10.005(10)	15.9169(15)	13.986(10)	9.6343(6)	17.979(2)
<i>b</i> (Å)	15.102(2)	10.721(11)	8.9235(9)	10.472(11)	23.0314(16)	11.0029(12)
<i>c</i> (Å)	22.205(3)	29.23(3)	19.8560(19)	17.895(14)	9.3407(6)	18.460(2)
α (deg)	90	89.09(2)	90	90	90	90
β (deg)	97.253(5)	82.05(3)	107.383(3)	90	112.419(3)	100.388(3)
γ (deg)	90	89.83(3)	90	90	90	90
volume (Å ³)	3452.2(8)	3104(5)	2691.4(5)	2621(4)	1916.0(2)	3591.9(7)
<i>Z</i>	4	2	4	4	4	4
<i>D</i> (calc, g/cm ³)	1.186	1.379	1.462	1.378	1.488	1.463
μ (mm ⁻¹)	0.804	0.899	1.034	0.852	1.143	0.678
<i>F</i> (000)	1296	1352	1224	1152	888	1648
2 θ _{max} (deg)	49.5	52.7	52.7	55.0	60.9	54.2
reflections collected	23622	47647	18059	14335	14816	29982
independent reflections	5845	12499	5457	5622	2908	7860
	(<i>R</i> _{int} = 0.0577)	(<i>R</i> _{int} = 0.0450)	(<i>R</i> _{int} = 0.0523)	(<i>R</i> _{int} = 0.0397)	(<i>R</i> _{int} = 0.0254)	(<i>R</i> _{int} = 0.0252)
observed reflections	4385 [<i>I</i> > 2 σ (<i>I</i>)]	9810 [<i>I</i> > 2 σ (<i>I</i>)]	4227 [<i>I</i> > 2 σ (<i>I</i>)]	5023 [<i>I</i> > 2 σ (<i>I</i>)]	2702 [<i>I</i> > 2 σ (<i>I</i>)]	6937 [<i>I</i> > 2 σ (<i>I</i>)]
goodness of fit	0.985	1.118	1.073	1.035	1.043	1.025
final <i>R</i> indices [<i>I</i> > 2 σ (<i>I</i>)]	<i>R</i> ₁ = 0.042, <i>wR</i> ₂ = 0.11	<i>R</i> ₁ = 0.0615, <i>wR</i> ₂ = 0.1344	<i>R</i> ₁ = 0.0508, <i>wR</i> ₂ = 0.1094	<i>R</i> ₁ = 0.0347, <i>wR</i> ₂ = 0.0728	<i>R</i> ₁ = 0.0228, <i>wR</i> ₂ = 0.0547	<i>R</i> ₁ = 0.0266, <i>wR</i> ₂ = 0.0625
absolute structure parameter				0.03(3)		

General Crystallographic Details. X-ray crystallography data were collected on a Bruker Nonius X8 Apex II CCD Diffractometer operating with MoK α radiation ($\lambda = 0.71073$ Å) at a temperature of 100(2) K. For *cis*-[RuCl(η^1 -N₂H₄)(depe)₂]⁺, **1a**, the routine SQUEEZE was applied to the data to remove diffuse electron density associated with disordered solvent that could not be modeled appropriately.²⁷ For *cis*-[RuCl(η^1 -N₂H₄)(depe)₂]⁺, **1b**, a number of restraints were applied to disordered groups within the structure. It was not possible to place H atoms on non-coordinating hydrazine molecules because of the presence of diffuse electron density, and some atoms were refined isotropically because of disorder. For complex *cis*-[Ru(η^1 -N₂H₄)₂(dmpe)₂]²⁺, **3**, the phosphine ligands were disordered over two positions, and these were modeled at partial occupancies. This disorder does not appear to affect the NH₂-NH₂ ligands bound to the metal center. In addition to this, there are two hydrazines of crystallization that are also disordered over either two or three positions, and these have also been modeled at partial occupancies. For complex [Ru(η^2 -NH=NH)(dmpe)₂], **5**, there is disorder present in the phosphine ligands around the Ru center, which have been successfully modeled at partial occupancies with the use of restraints. Crystallographic details for all compounds are summarized in Table 2.

***cis*-[RuCl(η^1 -N₂H₄)(depe)₂]⁺X⁻ 1.** X = Cl. *cis*-[RuCl₂(depe)₂] (110 mg, 0.188 mmol) was dissolved in a solution of hydrazine in tetrahydrofuran (1M, 1.5 mL, 1.5 mmol) under nitrogen to give a yellow solution. Diethyl ether (5 mL) was added and a pale yellow crystalline solid precipitated from the reaction mixture over several hours. *cis*-[RuCl(η^1 -N₂H₄)(depe)₂]⁺Cl⁻ **1** was collected by filtration and washed with diethyl ether (56 mg, 48% yield). ³¹P{¹H} NMR (MeOH, 121 MHz): δ 64.1 (ddd, ²*J*_{AB} 31.2 Hz, ²*J*_{AC} 17.1 Hz, ²*J*_{AD} 24.1 Hz, 1P, **P_A**), 54.9 (ddd, ²*J*_{BC} 26.4 Hz, ²*J*_{BD} 17.8 Hz, 1P, **P_B**), 48.1 (ddd, ²*J*_{CD} 278.4 Hz, 1P, **P_C**), 46.0 (ddd, 1P, **P_D**).

X = BPh₄. A solution of NaBPh₄ (56 mg, 0.16 mmol) in methanol (1 mL) was added to a solution of *cis*-[RuCl(η^1 -N₂H₄)(depe)₂]⁺Cl⁻ **1** (56 mg, 91 μ mol) in methanol (1 mL). The white precipitate formed was collected by filtration, washed with methanol and dried in vacuo to give *cis*-[RuCl(η^1 -N₂H₄)(depe)₂]⁺BPh₄⁻

1 (60 mg, 66 μ mol, 73%). C₄₄H₇₂BClN₂P₄Ru (900.39) requires C, 58.7; H, 8.1; N, 3.1; found C, 58.8; H, 8.1; N, 3.1%. ¹H NMR (thf-*d*₈, 400 MHz): δ 7.28 (m, 8H, *o*-Ph), 6.86 (m, 8H, *m*-Ph), 6.72 (m, 4H, *p*-Ph), 4.42 (br, 2H, RuNH₂), 3.74 (br, 2H, NH₂), 2.46 (m, 2H, CH₂), 2.20–1.31 (m, 22H, CH₂), 1.20 (m, 12H, CH₃), 1.09 (m, 12H, CH₃). ¹H{³¹P} NMR (thf-*d*₈, 400 MHz): δ 7.28 (m, 8H, *o*-Ph), 6.87 (m, 8H, *m*-Ph), 6.72 (m, 4H, *p*-Ph), 4.42 (br t, ³*J*_{HH} 4 Hz, 2H, RuNH₂), 3.74 (br t, ³*J*_{HH} 4 Hz, 2H, NH₂), 2.46 (m, 2H, CH₂), 2.20–1.31 (m, 22H, CH₂), 1.21 (m, 12H, CH₃), 1.09 (m, 12H, CH₃). ³¹P{¹H} NMR (thf-*d*₈, 162 MHz): δ 63.4 (ddd, ²*J*_{AB} 31.1 Hz, ²*J*_{AC} 17.1 Hz, ²*J*_{AD} 23.9 Hz, 1P, **P_A**), 54.8 (ddd, ²*J*_{BC} 26.3 Hz, ²*J*_{BD} 17.7 Hz, 1P, **P_B**), 48.4 (ddd, ²*J*_{CD} 278.5 Hz, 1P, **P_C**), 45.2 (ddd, 1P, **P_D**). ¹⁵N{¹H} NMR (thf-*d*₈, 41 MHz, from HN-HSQC): δ -318.5 (corr with ¹H δ 3.74, NH₂), -370.8 (corr with ¹H δ 4.42, Ru-NH₂). IR: 3330 m, 3302w, 3053w, 3032w, 1613 m, 1595 m, 1580 m, 1417s, 1268w, 1170 m, 1134w, 1081 m, 1034s, 868 m, 843w, 817 m, 762 m, 750s, 735s, 706s, 683 m, 665 m, 610s cm⁻¹. MS (ESI, thf): *m/z* 582.139 [60%, (Ru(N₂H₄)(depe)₂Cl+H)⁺], 565.137 [100, Ru(NH₂)(depe)₂Cl⁺].

The ¹⁵N-labeled analogue [RuCl(η^1 -¹⁵N₂H₄)(depe)₂]⁺Cl⁻ was prepared in situ by dissolving *cis*-[RuCl₂(depe)₂] (33 mg, 56 μ mol) in a solution of ¹⁵N₂H₄ (approximately 0.5 M in thf, 0.4 mL, 0.2 mmol) and thf-*d*₈ (0.1 mL). ³¹P{¹H} NMR (thf/thf-*d*₈, 162 MHz): δ 62.7 (ddd, ²*J*_{AB} 29.8 Hz, ²*J*_{AC} 18.1 Hz, ²*J*_{AD} 23.0 Hz, 1P, **P_A**), 53.9 (dddd, ²*J*_{BC} 25.0 Hz, ²*J*_{BD} 19.9 Hz, ²*J*_{BN} 28.1 Hz, 1P, **P_B**), 47.9 (ddd, ²*J*_{CD} 287.2 Hz, 1P, **P_C**), 46.7 (ddd, 1P, **P_D**). ¹⁵N{¹H} NMR (thf/thf-*d*₈, 41 MHz): δ -322.9 (d, ¹*J*_{NN} 5 Hz, NH₂), -335.1 (s, free ¹⁵N₂H₄), -373.7 (dd, ²*J*_{NP} 28 Hz, ¹*J*_{NN} 5 Hz, Ru-NH₂). ¹⁵N NMR (thf/thf-*d*₈, 41 MHz): δ -322.9 (br s, NH₂), -335.1 (s, free ¹⁵N₂H₄), -373.7 (dd, ¹*J*_{NH} 72 Hz, ²*J*_{NP} 28 Hz, ¹*J*_{NN} 5 Hz, Ru-NH₂).

***cis*-[RuCl(η^1 -N₂H₄)(dmpe)₂]⁺X⁻ 2 and *cis*-[Ru(η^1 -N₂H₄)₂(dmpe)₂]²⁺·2X⁻ 3.** X = Cl. Methanol (0.4 mL) was added to a suspension of *cis*-[RuCl₂(dmpe)₂] (0.159 g, 0.337 mmol) in hydrazine (1 M in thf, 1.2 mL, 1.2 mmol) under nitrogen to give a very pale yellow solution. Diethyl ether (5 mL) was added, and a white crystalline solid precipitated from the reaction mixture over several hours. The product obtained was a mixture of *cis*-[RuCl(η^1 -N₂H₄)(dmpe)₂]⁺Cl⁻ **2** and *cis*-[Ru(η^1 -N₂H₄)₂(dmpe)₂]²⁺Cl⁻ **3** (in a ratio of approximately 5:1) and was collected by filtration and washed with diethyl ether (0.160 g). ³¹P{¹H} NMR (MeOH,

(27) Spek, A. L. *Acta Crystallogr.* 1990, A46, C34.

162 MHz): δ 53.0 (ddd, $^2J_{AB}$ 33.2 Hz, $^2J_{AC}$ 16.3 Hz, $^2J_{AD}$ 25.2 Hz, 1P, **P_A**, 2), 44.8 (app t, splitting 20 Hz, 2P, **3**), 43.5 (ddd, $^2J_{BC}$ 28.3 Hz, $^2J_{BD}$ 15.8 Hz, 1P, **P_B**, 2), 40.6 (ddd, $^2J_{CD}$ 296.0 Hz, 1P, **P_C**, 2), 34.2, (app t, 2P, **3**), 33.6 (ddd, 1P, **P_D**, 2).

The ^{15}N -labeled analogues $[\text{Ru}(\eta^1\text{-}^{15}\text{N}_2\text{H}_4)(\text{dmpe})_2]^+\text{Cl}^-$ and $[\text{Ru}(\eta^1\text{-}^{15}\text{N}_2\text{H}_4)_2(\text{dmpe})_2]^+2\text{Cl}^-$ were prepared in an analogous reaction with *cis*- $[\text{RuCl}_2(\text{dmpe})_2]$ (65 mg, 0.14 mmol) in $^{15}\text{N}_2\text{H}_4$ (approximately 0.5 M in thf, 1.0 mL, 0.5 mmol), methanol (0.3 mL) and diethyl ether (4 mL) (yield 62 mg).

A solution for ^{15}N NMR studies was prepared in situ by dissolving *cis*- $[\text{RuCl}_2(\text{dmpe})_2]$ (38 mg, 80 μmol) in a solution of $^{15}\text{N}_2\text{H}_4$ (approximately 0.5 M in thf, 0.4 mL, 0.2 mmol), methanol (0.1 mL), and thf- d_8 (0.1 mL). $^{31}\text{P}\{^1\text{H}\}$ NMR (methanol/thf/thf- d_8 , 162 MHz): δ 52.5 (ddd, $^2J_{AB}$ 32.3 Hz, $^2J_{AC}$ 16.3 Hz, $^2J_{AD}$ 25.3 Hz, 1P, **P_A**, 2), 44.6 (m, 2P, **3**), 43.2 (dddd, $^2J_{BC}$ 28.7 Hz, $^2J_{BD}$ 15.7 Hz, $^2J_{BN}$ 28.9 Hz, 1P, **P_B**, 2), 40.7 (ddd, $^2J_{CD}$ 299.4 Hz, 1P, **P_C**, 2), 34.2 (app t, splitting 20 Hz, 2P, **3**), 33.8 (ddd, 1P, **P_D**, 2). $^{15}\text{N}\{^1\text{H}\}$ NMR (methanol/thf/thf- d_8 , 41 MHz): δ -320.7 (br m, NH_2 , 2), -322.5 (br m, NH_2 , 3), -335.6 (s, free $^{15}\text{N}_2\text{H}_4$), -365.7 (m, Ru-NH $_2$, 3), -369.2 (m, Ru-NH $_2$, 2).

X = BPh₄. A solution of NaBPh₄ (85 mg, 0.25 mmol) in methanol (1.6 mL) was added to a solution containing a mixture of *cis*- $[\text{RuCl}(\eta^1\text{-N}_2\text{H}_4)(\text{dmpe})_2]^+\text{Cl}^-$ **2** and *cis*- $[\text{Ru}(\eta^1\text{-N}_2\text{H}_4)_2(\text{dmpe})_2]^+2\text{Cl}^-$ **3** (0.100 g) in methanol (0.4 mL). The white precipitate formed was collected by filtration, washed with methanol, and dried in vacuo (0.135 g). The white solid was extracted with thf (6 mL), and then filtered. *cis*- $[\text{RuCl}(\eta^1\text{-N}_2\text{H}_4)(\text{dmpe})_2]^+\text{Cl}^-$ **2** was isolated as a white solid by evaporation of the filtrate to dryness (29 mg, 36 μmol , 17% based on $\text{RuCl}_2(\text{dmpe})_2$) while complex **3** remained undissolved in thf (17 mg, 15 μmol , 7% based on $\text{RuCl}_2(\text{dmpe})_2$).

cis- $[\text{RuCl}(\eta^1\text{-N}_2\text{H}_4)(\text{dmpe})_2]^+\text{BPh}_4^-$ **2**. $\text{C}_{36}\text{H}_{56}\text{BClN}_2\text{P}_4\text{Ru} \cdot 0.25(\text{C}_6\text{H}_8\text{O})$ (806.10) requires C, 55.1; H, 7.3; N, 3.5; found C, 55.5; H, 7.7; N, 3.3%. ^1H NMR (thf- d_8 , 400 MHz): δ 7.28 (m, 8H, *o*-Ph), 6.86 (m, 8H, *m*-Ph), 6.72 (m, 4H, *p*-Ph), 4.51 (br, 2H, RuNH $_2$), 3.67 (br, 2H, NH $_2$), 1.95–1.75 (m, 4H, CH $_2$), 1.65 (m, 3H, CH $_3$), 1.62–1.33 (m, 4H, CH $_2$), 1.51 (m, 3H, CH $_3$), 1.48 (m, 3H, CH $_3$), 1.42 (m, 3H, CH $_3$), 1.37 (m, 3H, CH $_3$), 1.31 (m, 3H, CH $_3$), 1.27 (m, 3H, CH $_3$), 1.15 (m, 3H, CH $_3$). $^1\text{H}\{^{31}\text{P}\}$ NMR (thf- d_8 , 400 MHz): δ 7.28 (m, 8H, *o*-Ph), 6.86 (m, 8H, *m*-Ph), 6.72 (m, 4H, *p*-Ph), 4.51 (m, 2H, RuNH $_2$), 3.67 (t, $^2J_{\text{HH}}$ 5 Hz, 2H, NH $_2$), 1.95–1.75 (m, 4H, CH $_2$), 1.65 (s, 3H, CH $_3$), 1.62–1.33 (m, 4H, CH $_2$), 1.51 (s, 3H, CH $_3$), 1.48 (s, 3H, CH $_3$), 1.42 (s, 3H, CH $_3$), 1.37 (s, 3H, CH $_3$), 1.31 (s, 3H, CH $_3$), 1.27 (s, 3H, CH $_3$), 1.15 (s, 3H, CH $_3$). $^{31}\text{P}\{^1\text{H}\}$ NMR (thf- d_8 , 162 MHz): δ 51.6 (ddd, $^2J_{AB}$ 32.3 Hz, $^2J_{AC}$ 15.9 Hz, $^2J_{AD}$ 25.1 Hz, 1P, **P_A**), 43.8 (ddd, $^2J_{BC}$ 28.2 Hz, $^2J_{BD}$ 15.8 Hz, 1P, **P_B**), 40.5 (ddd, $^2J_{CD}$ 299.7 Hz, 1P, **P_C**), 33.9 (ddd, 1P, **P_D**). $^{15}\text{N}\{^1\text{H}\}$ NMR (thf- d_8 , 41 MHz, from HN-HSQC): δ -317.7 (corr with ^1H δ 3.67, NH $_2$), -366.1 (corr with ^1H δ 4.51, Ru-NH $_2$). ^1H NMR (dms- d_6 , 400 MHz): δ 7.19 (m, 8H, *o*-Ph), 6.93 (m, 8H, *m*-Ph), 6.80 (m, 4H, *p*-Ph), 5.29 (br m, 1H, RuNHH), 4.66 (br m, 1H, RuNHH), 3.78 (br, 2H, NH $_2$), 3.16 (m, thf), 2.09–1.79 (m, 4H, CH $_2$), 1.76 (m, thf), 1.75–1.66 (m, 2H, CH $_2$), 1.63 (m, 3H, CH $_3$), 1.60–1.41 (m, 2H, CH $_2$), 1.53 (m, 6H, 2 \times CH $_3$), 1.47 (m, 3H, CH $_3$), 1.38 (m, 3H, CH $_3$), 1.32 (m, 6H, 2 \times CH $_3$), 1.24 (m, 3H, CH $_3$). $^1\text{H}\{^{31}\text{P}\}$ NMR (dms- d_6 , 400 MHz): δ 7.19 (m, 8H, *o*-Ph), 6.93 (m, 8H, *m*-Ph), 6.80 (m, 4H, *p*-Ph), 5.29 (br d, $^2J_{\text{HH}}$ 11 Hz, 1H, RuNHH), 4.66 (br d, $^2J_{\text{HH}}$ 11 Hz, 1H, RuNHH), 3.78 (br, 2H, NH $_2$), 3.16 (m, thf), 2.09–1.79 (m, 4H, CH $_2$), 1.76 (m, thf), 1.75–1.66 (m, 2H, CH $_2$), 1.63 (s, 3H, CH $_3$), 1.60–1.41 (m, 2H, CH $_2$), 1.55 (s, 3H, CH $_3$), 1.52 (s, 3H, CH $_3$), 1.47 (s, 3H, CH $_3$), 1.38 (s, 3H, CH $_3$), 1.33 (s, 3H, CH $_3$), 1.32 (s, 3H, CH $_3$), 1.24 (s, 3H, CH $_3$). $^{31}\text{P}\{^1\text{H}\}$ NMR (dms- d_6 , 162 MHz): δ 53.6 (ddd, $^2J_{AB}$ 32.5 Hz, $^2J_{AC}$ 16.0 Hz, $^2J_{AD}$ 25.1 Hz, 1P, **P_A**), 44.4 (ddd, $^2J_{BC}$ 28.5 Hz, $^2J_{BD}$ 15.2 Hz, 1P, **P_B**), 42.3 (ddd, $^2J_{CD}$ 300.5 Hz, 1P, **P_C**), 35.2 (ddd, 1P, **P_D**). $^{15}\text{N}\{^1\text{H}\}$ NMR (dms- d_6 , 41 MHz, from HN-HSQC): δ -321.7 (corr with ^1H δ 3.78, NH $_2$), -373.5 (corr with ^1H δ 5.29

and 4.66, Ru-NH $_2$). IR: 3277w, 3052m, 3033m, 1598w, 1578m, 1421s, 1303m, 1282w, 1267w, 1242w, 1155m, 1131w, 1079w, 1062m, 1033w, 930s, 912m, 893m, 839m, 798w, 748m, 734s, 707s, 651m, 610s cm^{-1} .

cis- $[\text{Ru}(\eta^1\text{-N}_2\text{H}_4)_2(\text{dmpe})_2]^+2\text{BPh}_4^-$ **3**. ^{28}H NMR (dms- d_6 , 400 MHz): δ 7.18 (m, 16H, *o*-Ph), 6.92 (m, 16H, *m*-Ph), 6.79 (m, 8H, *p*-Ph), 5.71 (br m, 2H, RuNHH), 5.59 (br m, 2H, RuNHH), 3.60 (br, 4H, NH $_2$), 2.09–1.79 (m, 4H, CH $_2$), 1.71 (m, 2H, CH $_2$), 1.57 (m, 12H, CH $_3$), 1.49 (m, 2H, CH $_2$), 1.37 (m, 6H, CH $_3$), 1.31 (m, 6H, CH $_3$). $^1\text{H}\{^{31}\text{P}\}$ NMR (dms- d_6 , 400 MHz): δ 7.18 (m, 16H, *o*-Ph), 6.92 (m, 16H, *m*-Ph), 6.79 (m, 8H, *p*-Ph), 5.71 (br m, 2H, RuNHH), 5.59 (br m, 2H, RuNHH), 3.60 (br m, 4H, NH $_2$), 1.99 (m, 2H, CH $_2$), 1.88 (m, 2H, CH $_2$), 1.73 (m, 2H, CH $_2$), 1.58 (s, 6H, CH $_3$), 1.57 (s, 6H, CH $_3$), 1.49 (m, 2H, CH $_2$), 1.37 (s, 6H, CH $_3$), 1.31 (s, 6H, CH $_3$). $^{31}\text{P}\{^1\text{H}\}$ NMR (dms- d_6 , 162 MHz): δ 45.7 (app t, splitting 20 Hz, 2P), 35.5 (app t, 2P). $^{15}\text{N}\{^1\text{H}\}$ NMR (dms- d_6 , 41 MHz, from HN-HSQC): δ -322.7 (corr with ^1H δ 3.60, NH $_2$), -368.0 (corr with ^1H δ 5.71 and 5.59, Ru-NH $_2$).

cis- $[\text{Ru}(\eta^2\text{-NH=NH})(\text{depe})_2]^+\text{Cl}^-$ **1**. A suspension of *cis*- $[\text{RuCl}(\eta^1\text{-N}_2\text{H}_4)(\text{depe})_2]^+\text{Cl}^-$ **1** (0.196 g, 0.318 mmol) and KO^tBu (0.101 g, 0.900 mmol) was stirred in thf (10 mL) under argon for 40 min, and then the solvent was removed under reduced pressure. The residue was extracted with pentane (45 mL), filtered through Celite, and the filtrate evaporated to dryness under reduced pressure to afford an off-white solid. Slow crystallization from benzene and then washing with pentane afforded yellow crystals (63.0 mg, 0.116 mmol, 36% yield). $\text{C}_{20}\text{H}_{50}\text{N}_2\text{P}_4\text{Ru}$ (543.59) requires C, 44.2; H, 9.3; N, 5.2; found C, 44.1; H, 9.4; N, 4.5%. ^1H NMR (thf- d_8 , 400 MHz): δ 2.31 (br, 2H, RuNH), 2.03 (m, 2H, CH $_2$), 1.84–1.64 (m, 4H, CH $_2$), 1.56 (m, 10H, CH $_2$), 1.37 (m, 4H, CH $_2$), 1.21 (m, 4H, CH $_2$), 1.14 (m, 6H, CH $_3$), 1.06 (m, 6H, CH $_3$), 0.97 (m, 12H, CH $_3$). $^1\text{H}\{^{31}\text{P}\}$ NMR (thf- d_8 , 400 MHz): δ 2.31 (br, 2H, RuNH), 2.03 (m, 2H, CH $_2$), 1.84–1.64 (m, 4H, CH $_2$), 1.56 (m, 10H, CH $_2$), 1.37 (m, 4H, CH $_2$), 1.21 (m, 4H, CH $_2$), 1.14 (t, $^3J_{\text{HH}}$ 8 Hz, 6H, CH $_3$), 1.06 (t, $^3J_{\text{HH}}$ 8 Hz, 6H, CH $_3$), 0.97 (m, 12H, CH $_3$). $^{31}\text{P}\{^1\text{H}\}$ NMR (thf- d_8 , 162 MHz): δ 61.7 (app t, splitting 25 Hz, 2P), 57.5 (app t, 2P). IR (nujol): 3210s, 2723w, 1416s, 1263w, 1244m, 1198m, 1074m, 1038s, 1025s, 982s, 872m, 810s, 749s, 733s, 720s, 704s, 655s, 633s, 618s cm^{-1} .

Compound **4** can also be synthesized in an analogous fashion by treating *cis*- $[\text{RuCl}(\eta^1\text{-N}_2\text{H}_4)(\text{depe})_2]^+\text{Cl}^-$ **1** (0.219 g, 0.355 mmol) with $\text{K}[\text{N}(\text{SiMe}_3)_2]$ (0.156 g, 0.782 mmol). Yield 52.3 mg (27%).

The ^{15}N -labeled analogue *cis*- $[\text{Ru}(\eta^2\text{-}^{15}\text{NH}=\text{NH})(\text{depe})_2]^+$ was prepared in an analogous reaction by treating a solution of $[\text{RuCl}(\eta^1\text{-}^{15}\text{N}_2\text{H}_4)(\text{depe})_2]^+\text{Cl}^-$ in thf and thf- d_8 with KO^tBu (19 mg, 0.17 mmol). The reaction mixture was evaporated to dryness under reduced pressure. The residue was extracted with pentane (3 \times 2 mL), filtered through Celite, and the filtrate evaporated to dryness under reduced pressure to afford a pale yellow tacky solid. $^{31}\text{P}\{^1\text{H}\}$ NMR (thf- d_8 , 162 MHz): δ 61.8 (app tt, splitting 25 Hz, 4 Hz, 2P), 57.3 (app t, splitting 25 Hz, 2P). $^{15}\text{N}\{^1\text{H}\}$ NMR (thf- d_8 , 41 MHz): δ -313.7 (br). ^{15}N NMR (thf- d_8 , 41 MHz): δ -313.7 (br).

cis- $[\text{Ru}(\eta^2\text{-NH=NH})(\text{dmpe})_2]^+\text{Cl}^-$ **5**. A suspension of *cis*- $[\text{RuCl}(\eta^1\text{-N}_2\text{H}_4)(\text{dmpe})_2]^+\text{Cl}^-$ **2** (0.200 g, 0.397 mmol)³⁰ and KO^tBu (0.103 g, 0.918 mmol) was stirred in thf (20 mL) under argon for 50 min, filtered through Celite, and the filtrate evaporated to dryness under vacuum. The residue was extracted with benzene

(28) Satisfactory microanalysis not obtained because of small amount of complex **2** present in the material.

(29) Microanalyses conducted for ruthenium diazene complexes consistently returned low values for N even for crystalline samples of these complexes. We attribute this to facile loss of the diazene from the complex during the analysis process. The same phenomenon was apparent in microanalysis of iron-diazenes.

(30) This material contained a small amount of *cis*- $[\text{Ru}(\text{N}_2\text{H}_4)_2(\text{dmpe})_2]^+2\text{Cl}^-$ **3**.

(20 mL) and evaporated to dryness under reduced pressure to afford a pale orange solid. Slow crystallization from benzene and then washing with small amounts of benzene afforded nearly colorless crystals (13.5 mg, 31.3 μmol , 8% yield). $\text{C}_{12}\text{H}_{34}\text{N}_2\text{P}_4\text{Ru}$ (431.43) requires C, 33.4; H, 8.0; N, 6.5; found C, 33.7; H, 8.2; N, 5.8%. ^{1}H NMR (benzene- d_6 , 400 MHz): δ 2.96 (br, 2H, RuNH), 1.64–1.44 (m, 2H, CH_2), 1.41 (m, 6H, CH_3), 1.39–1.16 (m, 4H, CH_2), 1.12 (m, 6H, CH_3), 1.03 (m, 6H, CH_3), 0.92 (m, 8H, CH_2 and 2 \times CH_3). $^1\text{H}\{^{31}\text{P}\}$ NMR (benzene- d_6 , 400 MHz): δ 2.96 (br, 2H, RuNH), 1.49 (m, 2H, CH_2), 1.41 (s, 6H, CH_3), 1.35 (m, 2H, CH_2), 1.25 (m, 2H, CH_2), 1.12 (s, 6H, CH_3), 1.03 (s, 6H, CH_3), 0.92 (m, 8H, CH_2 and 2 \times CH_3). $^{31}\text{P}\{^1\text{H}\}$ NMR (benzene- d_6 , 162 MHz): δ 41.4 (app t, splitting 24 Hz, 2P), 39.2 (app t, 2P). IR (nujol): 3195w, 2794w, 1413m, 1288m, 1272m, 1227w, 1194s, 1115w, 1063w, 993m, 942s, 923s, 885s, 831s, 789m, 724m, 703s, 684s, 640s cm^{-1} .

The ^{15}N -labeled analogue *cis*- $[\text{Ru}(\eta^2\text{-}^{15}\text{NH}=\text{NH})(\text{dmpe})_2]$ was prepared in an analogous reaction by treating a solution of $[\text{RuCl}(\eta^1\text{-}^{15}\text{N}_2\text{H}_4)(\text{dmpe})_2]^+\text{Cl}^-$ (32 mg, 63 μmol) in thf (1.5 mL) and thf- d_8 (0.7 mL) with KO^tBu (37 mg, 0.33 mmol) and then the reaction mixture was evaporated to dryness under reduced pressure. The residue was extracted with pentane (3 \times 1 mL, 3 \times 2 mL), filtered through Celite, and the filtrate evaporated to dryness under reduced pressure to afford a pale yellow-orange tacky solid. $^{31}\text{P}\{^1\text{H}\}$ NMR (thf- d_8 , 162 MHz): δ 41.4 (app t, splitting 26 Hz, 2P), 39.8 (app t, splitting 26 Hz, 2P). $^{15}\text{N}\{^1\text{H}\}$ NMR (thf- d_8 , 41 MHz): δ -312.2 (t, $^2J_{\text{NP}}$ 4.5 Hz). ^{15}N NMR (thf- d_8 , 41 MHz): δ -312.2 (t, $^2J_{\text{NP}}$ 4.5 Hz).

cis- $[\text{Ru}(\eta^2\text{-N}_2\text{H}_4)(\text{depe})_2]^{2+} \cdot 2\text{X}^- \mathbf{6}$. **X = OTf.** *cis*- $[\text{Ru}(\eta^2\text{-NH}=\text{NH})(\text{depe})_2]$ (48.6 mg, 89.4 μmol) and lutidinium triflate (50.6 mg, 0.197 mmol) were dissolved in tetrahydrofuran (0.6 mL) under argon to give a yellow solution. Diethyl ether (2.5 mL) was added, and the reaction mixture left to stand overnight. The yellow crystals formed were collected by filtration and washed with diethyl ether (60 mg, 80% yield). ^1H NMR (thf- d_8 , 400 MHz): δ 5.89 (br, 2H, RuNHH), 5.29 (br, 2H, RuNHH), 3.62 (m, thf), 2.28–1.64 (m, 24H, CH_2 and thf), 1.20

(m, 18H, CH_3), 1.08 (m, 6H, CH_3). $^1\text{H}\{^{31}\text{P}\}$ NMR (thf- d_8 , 400 MHz): δ 5.89 (br, 2H, RuNHH), 5.29 (br, 2H, RuNHH), 3.62 (m, thf), 2.28–1.64 (m, 24H, CH_2 and thf), 1.21 (t, $^3J_{\text{HH}}$ 7 Hz, 12H, CH_3), 1.18 (t, $^3J_{\text{HH}}$ 7 Hz, 6H, CH_3), 1.09 (t, $^3J_{\text{HH}}$ 7 Hz, 6H, CH_3). $^{31}\text{P}\{^1\text{H}\}$ NMR (thf- d_8 , 162 MHz): δ 70.7 (app t, splitting 20 Hz, 2P), 50.1 (app t, splitting 20 Hz, 2P). $^{15}\text{N}\{^1\text{H}\}$ NMR (thf- d_8 , 41 MHz, from HN-HSQC): δ -378.7 (corr with ^1H δ 5.89 and 5.29, Ru-NH₂). ^{19}F NMR (thf- d_8 , 376 MHz): δ -79.1 (s, SO_3CF_3). IR: 3269m, 3219m, 3165m, 1641w, 1626m, 1598m, 1425m, 1265s, 1223s, 1148s, 1087w, 1060w, 1030s, 904w, 871w, 809w, 758m, 738m, 722m, 636s, 572s cm^{-1} . MS (ESI, thf): m/z 617.214 [100%, $(\text{Ru}(\text{N}_2\text{H}_4)(\text{depe})_2+\text{thf})^+$], 576.162 [25, $(\text{Ru}(\text{N}_2\text{H}_4)(\text{depe})_2+\text{OMe})^+$].

X = BF₄. *cis*- $[\text{Ru}(\eta^2\text{-NH}=\text{NH})(\text{depe})_2]$ (33.5 mg, 61.6 μmol) and lutidinium tetrafluoroborate (24.5 mg, 0.126 mmol) were suspended in tetrahydrofuran (0.6 mL) under. On standing for several hours, yellow needles formed which were collected by filtration and washed with diethyl ether (13 mg, 29% yield). $\text{C}_{20}\text{H}_{52}\text{B}_2\text{F}_8\text{N}_2\text{P}_4\text{Ru} \cdot 0.5(\text{C}_4\text{H}_8\text{O})$ (755.37) requires C, 35.0; H, 7.5; N, 3.7; found C, 35.3; H, 7.3; N, 3.7%. ^1H NMR (dms o - d_6 , 400 MHz): δ 6.13 (br, 2H, RuNHH), 5.30 (br, 2H, RuNHH), 3.60 (m, thf), 2.13–1.41 (m, 24H, CH_2 and thf), 1.08 (m, 18H, CH_3), 0.94 (m, 6H, CH_3). $^1\text{H}\{^{31}\text{P}\}$ NMR (dms o - d_6 , 400 MHz): δ 6.13 (br, 2H, RuNHH), 5.30 (br, 2H, RuNHH), 3.60 (m, thf), 2.13–1.41 (m, 24H, CH_2 and thf), 1.08 (m, 18H, CH_3), 0.94 (t, $^3J_{\text{HH}}$ 7 Hz, 6H, CH_3). $^{31}\text{P}\{^1\text{H}\}$ NMR (dms o - d_6 , 162 MHz): δ 72.0 (app t, splitting 20 Hz, 2P), 51.9 (app t, splitting 20 Hz, 2P). $^{15}\text{N}\{^1\text{H}\}$ NMR (dms o - d_6 , 41 MHz, from HN-HSQC): δ -379.1 (corr with ^1H δ 6.13 and 5.30, Ru-NH₂). ^{19}F NMR (dms o - d_6 , 376 MHz): δ -148.26 (s, $^{10}\text{BF}_4$), -148.31 (s, $^{11}\text{BF}_4$).

Acknowledgment. We gratefully acknowledge financial support from the Australian Research Council.

Supporting Information Available: CIF files for **1a**, **1b**, **3**, **4**, **5**, and **6**. This material is available free of charge via the Internet at <http://pubs.acs.org>.